Defining the critical state line from triaxial compression and ring shear tests

Définition de l'état critique ligne à partir des tests de compression triaxiale et de cisaillement circulaire

A. Sadrekarimi
Department of Civil & Environmental Engineering, University of Illinois at Urbana-Champaign, Urbana, IL USA

S.M. Olson
Department of Civil & Environmental Engineering, University of Illinois at Urbana-Champaign, Urbana, IL USA

ABSTRACT
The critical state (or critical void ratio) line is the locus of void ratio-effective stress conditions achieved after shearing a soil to large displacement and after all net void ratio changes and effective stress changes are complete. The triaxial compression test is commonly used to define the critical state line of sandy soils. In this study, we present drained and undrained triaxial compression and ring shear tests that are used to define the critical state line of a silty sand sampled from the Mississippi River near Cape Girardeau, Missouri, USA. All specimens were prepared by pluviating the dry sand through air. The results show that both drained and undrained (or constant volume) triaxial and ring shear tests reach critical state at similar shear displacements prior to the onset of particle damage in the ring shear tests. A unique critical state line can be defined for these states. At larger shear displacements only possible in the ring shear tests, considerable particle crushing happens and dominates the sand behavior and only after very large shear displacements (> 750 cm) particle crushing ceases to continue and a complete particle rearrangement is reached. At this state, the stresses and volume of the sand become constant which corresponds to the critical state of the crushed sand. A unique line can also be drawn for this state. These unique critical state lines indicate that they are not influenced by the drainage conditions and shearing modes.

RÉSUMÉ
Le état critique (ou plutôt le coefficient de vide critique) est le lieu où s'effectuent les conditions vides du rapport d'élasticité manifestées après des effets de cisaillement ayant causé des déplacements des sols et après que tous les changements de proportions vides et que les changements efficaces d'élasticité soient complets. Le test de compression triaxiale est couramment utilisé pour définir le état critique des sols sableux. Dans cette étude, nous présenterons des tests de compression triaxiale et de cisaillement circulaire drainés et détrempés utilisés dans la définition du état critique à partir de prélevements de sols vaseux naturels du fleuve Mississippi à proximité du Cap Girardeau, dans le Missouri aux Etats-Unis. Tous les spécimens ont été préparés en arrosant d'eaux de pluie le sable sec dans l'air. Les résultats montrent que tant égoutté que non égoutté (ou le volume constant) triaxial et les épreuves de tondage d'anneau atteignent l'état critique aux déplacements de tondage semblables avant le commencement de dommage de particule dans les épreuves de tondage d'anneau. Nous pouvons donc déterminer un état critique unique pour ces états. Lors de mouvements de cisaillements plus larges, possibles uniquement dans la cadre de tests, on peut observer un concassage intense de particules qui domine alors la texture du sable. Ce n'est qu'après de larges déplacements dûs aux mouvements de cisaillement (environ 750 cm) que cesse l'écrasement des particules et que l'ensemble des particules a subi une réorganisation complète. L'élasticité et le volume du sable deviennent alors constants, ce qui signale alors que le état critique du sable de concassage a été atteint. On peut également tracer une ligne unique de cette formation. Ces limites critiques indiquent qu'elles ne sont pas influencées par les conditions de drainage et les modes de cisaillement.

Keywords : sand, critical state, ring shear, triaxial shear, undrained, constant volume.

1 INTRODUCTION

Casagrande (1936) first observed that loose and dense sand specimens sheared under drained conditions achieved an essentially constant porosity that was independent of the initial condition. Taylor (1948) termed the corresponding void ratio that the specimen achieved when sheared to a constant volume and constant shear resistance condition the critical void ratio. Roscoe et al. (1958) extended Casagrande's concept of critical void ratio to the critical void ratio state at which any further increment of shear deformation would not result in any void ratio change in a drained test or would not result in any change in effective stress and shear resistance in an undrained test. In sands, the critical state typically occurs at large strains when the volume, porewater pressure, and shear and normal stresses remain constant. The ring shear (RS) apparatus was designed initially to investigate the critical shear resistance (i.e., residual strength) of clays (e.g., Bishop et al. 1971; Bromhead 1979) because of its ability to reach large shear displacements – a typical requirement for reaching critical state conditions. In this paper, we present results from monotonically-loaded RS tests to evaluate the critical state of a silty sand. The results are compared with critical states interpreted from monotonically-loaded triaxial compression (TxC) tests. Following the precedent set by many previous researchers (e.g. Poorooshasb 1989; Been et al. 1991; Verdugo and Ishihara 1996; Riemer and Seed 1997; Jang and Frost 2000), we use a single term "critical state" to describe critical state, steady state, residual state, and ultimate state of sands (Roscoe et al. 1958; Poulos 1981; Infante Sedano 1998; Iverson et al. 1998).

2 EXPERIMENTAL PROGRAM

Mississippi River (MR) sand is very fine-grained alluvial silty sand with an average fines content of 38% that we sampled near Cape Girardeau, Missouri. It has subangular to subrounded particles, and contains about 70% albite, 21% quartz (both

Proceedings of the 17[th] International Conference on Soil Mechanics and Geotechnical Engineering
M. Hamza et al. (Eds.)

doi:10.3233/978-1-60750-031-5-36

determined by X-ray diffraction), 5% calcite (determined by acid dissolution), and 4% various other minerals. Its G_s = 2.65 (ASTM D854-00), e_{max} = 1.038, and e_{min} = 0.563 (Yamamuro and Lade 1997).

We used air pluviation to prepare TxC and RS specimens for this study. For the TxC specimens, dry sand was poured into a funnel with its tip resting on the bottom of the specimen mold. The funnel was gently raised to deposit the particles. After placing the sand in the triaxial split mold, we leveled the top of the specimen using a straight-edge and placed the filter paper and porous steel disc on top of the specimen. We then set the top cap in place and rolled the membrane over the top cap. To minimize end restraint, we lubricated the end platens using a thin layer of silicon grease. We applied a vacuum of approximately 20 kPa to maintain the specimen shape while removing the split mold. After removing the mold, we measured the specimen dimensions with a caliper and weighed the remaining soil (not used during specimen preparation). These procedures allowed us to compute the initial void ratio of the sample with an average accuracy of ±0.005 (Sadrekarimi 2009). We then assembled the confining cell and filled the cell with silicon oil and applied a confining pressure of approximately 20 kPa while releasing the vacuum. We followed the backpressure saturation procedure to dissolve any remaining air and saturate the specimen until we observed a pore pressure parameter (B) of at least 0.97. Care was taken to ensure that the effective stress on the specimen never exceeded approximately 20 kPa while preparing each specimen and the triaxial device's data acquisition system recorded any volume changes. Following preparation, we consolidated each specimen to the target consolidation pressure (σ'_c) at a rate of 13.8 kPa/min. After consolidation, the drainage lines were closed or opened for undrained or drained shearing, respectively. We then sheared the specimen at a rate of 0.127 cm/min to an axial strain of 25%. Corrections were made to the measured stresses to account for the increased specimen area (Bishop and Henkel 1962).

In an RS test, an annular specimen is confined between outer and inner rings and is sheared at its bottom surface (or top or midheight depending on the configuration and fixity of the rings). A fixed plate on the top surface measures the specimen's resistance to shearing. Sadrekarimi and Olson (2009) summarize the advantages that the shears test provides for measuring the large displacement shearing resistance of sands. Constant volume and drained RS tests were performed using the newly developed solid confining rings type RS apparatus designed and built at the University of Illinois (Sadrekarimi and Olson 2009). All tests were performed on dry air pluviated sand where the specimens were not saturated. The ring shear apparatus has inner and outer diameters of 20.3 cm and 27.0 cm, respectively, and a height of 2.6 cm. The ratio of the outer to inner ring diameter is 1.33. This diameter ratio results in an error of less than 3% at the peak shear stress due to strain non-uniformity (Hvorslev 1939). The wide sample section (3.3 cm) also minimizes wall friction effects. Each ring shear specimen was deposited in the ring shaped chamber of the apparatus, consolidated to the target consolidation normal stress (σ'_c), and sheared at a rate of 18.6 cm/min. The dry mass and height of the specimen were used to define the global void ratios with an average accuracy of ±0.007 (Sadrekarimi 2009). A constant volume condition was imposed by locking the loading plates of the apparatus after consolidating the specimen and shearing was induced by rotating the bottom disk, which was deeply serrated to prevent slippage. For drained testing, the loading plate was left free to move up and down. Sadrekarimi and Olson (2009) provide further detail of the RS device, specimen preparation, and testing methods. Table 1 provides the consolidation conditions for each of the TxC and RS tests performed for this study.

Table 1. Consolidation conditions of the TxC and RS tests

TxC tests[1]	σ'_c (kPa)[2]	Dr_c (%)[3]	RS tests[1]	σ'_c (kPa)[2]	Dr_c (%)[3]
TXUN32	221	68	RSCV57	378	59
TXUN62	425	85	RSCV43	298	69
TXUN92	636	93	RSCV87	602	70
TXUN47	326	84	RSCV89	624	57
TXUN39	272	83	RSCV103	728	76
TXUN58	397	80	RSCV97	708	88
TXUN23	161	67	RSCV22	151	65
TXDR29	200	73	RSCV48	355	87
TXDR29	200	69	RSDR39	271	63
TXDR16	109	60	RSDR4	28	56
TXDR81	560	80	RSDR40	276	67
TXDR64	443	72	RSDR77	523	73
TXDR41	281	79	RSCV57	378	59

[1]TX and RS indicate triaxial compression and ring shear tests, respectively. UN, CV, and DR indicate undrained, constant volume, or drained conditions, respectively.
[2] σ'_c is the consolidation normal stress (σ'_n) in the RS tests and consolidation mean stress (σ'_{mean}) in the TxC tests.
[3] Relative density after consolidation.

3 EXPERIMENTAL RESULTS

Figures 1 through 4 present typical stress paths and stress–displacement plots for some of the experiments performed in this study. Deviator stress ($\sigma_1 - \sigma_3$) and shear stress (τ) are used in the stress paths of TxC and RS tests, respectively. In order to make clear comparisons, displacements (shear displacement in RS and axial displacement in TxC) rather than strains are used to illustrate the test results. Sadrekarimi (2009) presents the results of all of the tests listed in Table 1.

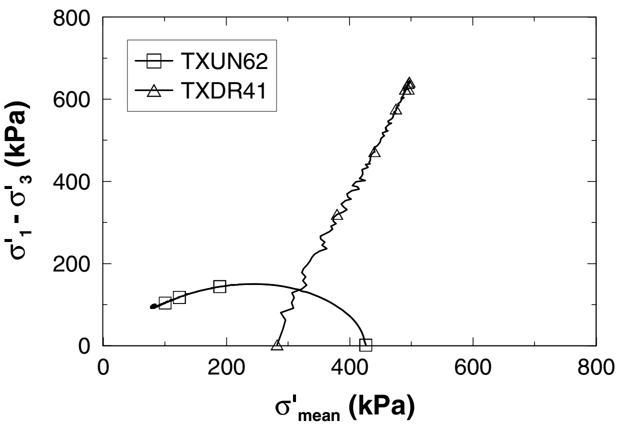

Figure 1. Example stress paths of TxC tests on air pluviated MR sand

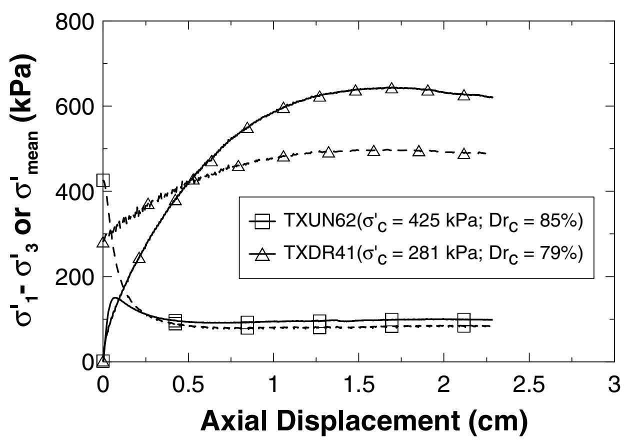

Figure 2. Example stress-displacement plots of TxC tests on air pluviated MR sand (σ'_1 - σ'_3 = solid line; σ'_{mean} = dashed line) - σ'_c is the consolidation mean stress.

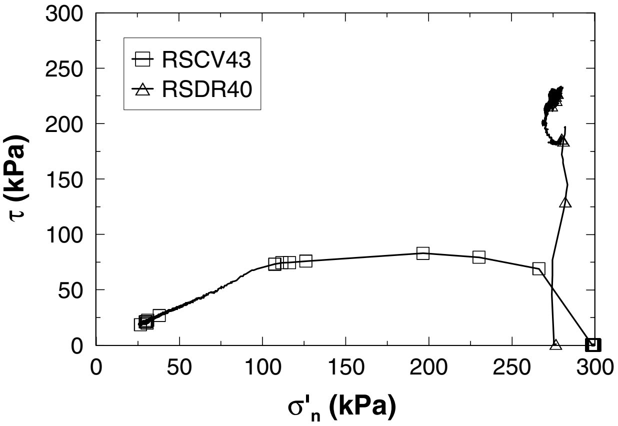

Figure 3. Example stress paths of RS tests on air pluviated MR sand

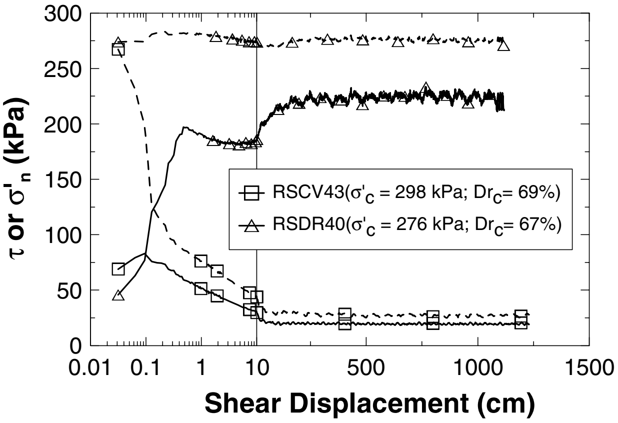

Figure 4. Example stress-displacement plots of RS tests on air pluviated MR sand (τ = solid line; σ'_n = dashed line) - σ'_c is the consolidation normal stress.

Both undrained and drained triaxial specimens of MR sand were contractive and a constant state was reached at average shear displacements of 0.75 cm and 1.6 cm, respectively. However, after shear displacements of 1.0 cm and 1.75 cm in undrained and drained tests, respectively, the deviator stresses tended to increase slightly in the undrained TxC tests and decrease slightly in the drained tests. But the limited displacement capacity of the triaxial device made it impossible to reliably measure soil response at axial displacements > 2.5 cm and to confidently assess the critical state.

In the RS experiments (Figs. 3 and 4), constant shear and normal stresses were reached after about 175 cm of shear displacement. This condition was maintained to more than 10 m of shear displacement, indicating a true critical state. Well-defined shear bands developed in the RS tests at the maximum mobilized shear resistance (at a shear displacement of 5.3 mm), after which the shear deformations were concentrated in the shear band and the soil above the shear band remained stationary (Sadrekarimi 2009). Void ratio changes after shear band formation occurred solely within the shear band. This indicates that the local void ratio within the shear band would differ from the global void ratio, and the local shear band void ratio should be measured and used to describe the specimen state (e.g. Finno et al 1996; Frost and Jang 2000). In this study global void ratios were computed using a linear voltage displacement transducer (LVDT) in the RS and TxC tests. In the RS tests, local void ratio changes in the shear band result from grain crushing and particle rearrangement. This was manifested externally by specimen height changes and system compliance. Sadrekarimi (2009) developed an analytical method to estimate local void ratio in the shear band.

4 DISCUSSION

Figure 5 shows the critical state lines of MR sand from TxC and RS tests. Local void ratios were used to define the critical state lines (CSL) from the RS results while global void ratios were used for TxC tests. For the RS tests, the effective normal stress on the shear surface (σ'_n) was used rather than the effective mean stress (σ'_{mean}) because principal stresses are not controlled or measured in RS tests. In contrast, the shear and effective normal stress on the failure plane can be computed readily in TxC tests for a theoretical failure plane at (45 - $\phi'/2$) with respect to the major principal stress plane (e.g. Holtz and Kovacs 1981) where ϕ' is the critical state friction angle of the sand (= 39° for MR sand; Sadrekarimi 2009). The void ratio and σ'_n at an axial displacement of 2.5 cm (which corresponds to a shear displacement of 2.8 cm on the failure plane) were used to construct the TxC CSL, after which the specimen severely bulged and the element test results became unreliable. For comparison, the critical state lines from the RS tests are drawn for 2.8 cm of shear displacement and for the shear displacement at the end of the tests (> 1000 cm).

As shown in Figure 5, a single CSL was obtained from the TxC and RS tests on MR sand at 2.8 cm of shear displacement, independent of the drainage conditions and mode of shear. Furthermore, the contractive response of both TxC and RS specimens (see Figs. 1 - 4) suggest that relatively small shear displacements may be sufficient for complete particle rearrangement. In addition, we observed negligible crushing in TxC and RS specimens after 2.8 cm of displacement (Sadrekarimi 2009). Thus the response observed at 2.8 cm of shear displacement represents a CSL of the original MR sand gradation, termed the CSL_o. The scatter in the state data at 2.8 cm displacement is the result of the uncertainty in determining the local shear band void ratio determination in the RS tests because of the very fine sand gradation and the resulting thin shear band, as well as the possibility of internal shear banding in the TxC specimens (particularly the denser specimens) that was not visible on the specimen outer surface.

As shearing continued, severe particle damage and crushing (as observed by comparing the before and after shearing particle size distributions of the sand) occurred within the shear band and local void ratio continued to decrease well beyond the displacement capacity of any other typical soil mechanics laboratory test devices (e.g., triaxial, simple shear, and direct shear). A constant global volume was reached in all of the RS tests only after very large shear displacements (> 700 cm) when the potential for particle crushing and contraction was essentially exhausted and the soil reached a stable grading (Coop et al. 2004). The fine angular grains produced by crushing caused the critical state line to become steeper (Castro 1969; Been and Jefferies 1985). Furthermore, the more efficient particle packing resulting from the broader grain size distribution of the crushed sand within the shear band caused the shear band critical state line to shift downward in e – log σ'_n space (Dawson et al. 1994).

After about 700 cm of shear displacement, a state of constant shear stress, constant effective normal stress, and constant void ratio was reached in all of the RS tests, indicating that a true critical state was attained. The locus of these critical states was termed the critical state line of the crushed sand (CSL_c). The unique critical state lines (CSL_o and CSL_c) from both drained and constant volume (or undrained) RS and TxC tests indicates that critical states corresponding to complete particle rearrangement (CSL_o) and complete particle crushing and rearrangement (CSL_c) are independent of drainage conditions (Been et al. 1991; Murthy et al. 2007), mode of shear (Poulos 1981), and consolidation stress. This further suggests that critical state and steady state (Poulos 1981) are the same.

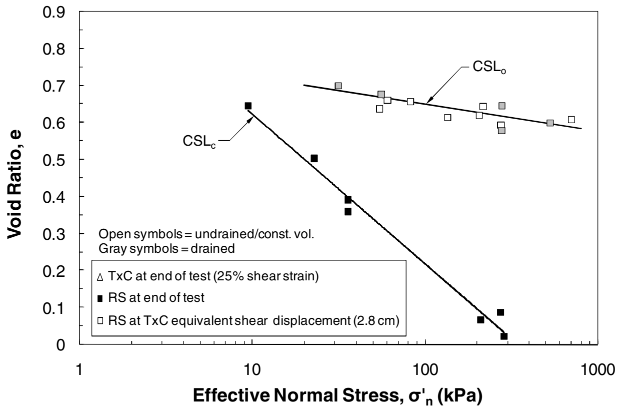

Figure 5. CSL_o and CSL_c from shears and TxC tests.

5 CONCLUSION

The determination and overall validity of the critical state in sand is of considerable importance, as it provides the basis for failure criteria of many constitutive models, and is a useful framework for comparing laboratory tests and field observations. By far, the triaxial device has been most widely employed to study the critical state of sands. However, the limited displacement that the triaxial device is capable of imposing on a specimen often is insufficient to reach a critical state where particle rearrangement and potential crushing are complete. As a result, studies using the triaxial device have yielded contradictory conclusions regarding the uniqueness of the critical state line (CSL) and the role of factors such as stress path, mode of shear, and consolidation stress on the CSL.

In this study, we performed a suite of ring shear (RS) tests on a silty sand using a newly designed RS device constructed at the University of Illinois to examine the critical state. The results of these tests demonstrate that shear band formation and particle damage play an important role in the contractive response of sands, and led us to propose two types of critical states. The CSL_o (critical state line of the original sand gradation without crushing) is achieved solely through particle reorientation/rearrangement. In this case, liquefaction and undrained post-peak strain-softening leading to the critical state occurs only in contractive sands and can be achieved at small shear displacements (about 2.8 cm for the sand tested in this study) within the capacity of nearly all laboratory testing devices, including the triaxial and simple shear devices. In contrast, the CSL_c (critical state line including particle damage and crushing) involves shear band formation and particle damage/crushing within the shear band. In this case, very large displacements (on the order of meters) are required to reach a critical state and this level of shear displacement can only be achieved in an RS device. Both CSL_o and CSL_c reflect the mineralogy of the sand and are independent of drainage conditions and consolidation stress, with the former being independent of the mode of shear as well.

REFERENCES

Been, K., Jefferies, M. G. and Hachey, J. 1991. The critical state of sands. Geotechnique, Vol.41, No.3, pp.365-381.

Been, K., and Jefferies, M. G. 1985. A state parameter for sands, Geotechnique, Vol.35, No.2, pp.99-112.

Bishop, A. W, Green, GE, Garga, V.K., Andersen, A, and Browns, J.D. 1971. A new ring shear apparatus and its application to the measurement of residual strength. Geotechnique, Vol.21, No.4, pp.273–328.

Bishop, A. W., and Henkel, D. J. 1962. *The measurement of soil properties in the triaxial test*. Edward Arnold, London.

Bromhead, E.N. 1979. A simple ring shear apparatus. Ground Engineering, Vol.12, No.5, pp.40-44.

Casagrande, A. 1936. Characteristic of cohesionless soils affecting the stability of slopes and earth fills, Journal of Boston Society of Civil Engineers, Vol.23, No.1,pp.13-32.

Castro, G. 1969. Liquefaction of sands, Ph.D. Dissertation, Harvard University, Cambridge, Massachusetts.

Coop, M. R., Sorensen, K. K., Bodas Freitas, T. and Georegoutos, G. 2004. Particle breakage during shearing of a carbonate sand, Geotechnique, Vol.54, No.3, pp.157-163.

Dawson, R.F., Morgenstern, N.R. and Gu, W. H. 1994. Liquefaction flowslides in Western Canadian coal mine waste dumps – Phase II: case histories, Energy, Mines, and Resources Canada, Ottawa.

Finno, R.J., Harris, W., Mooney, M., Viggiani, G. 1996. Strain localization and undrained steady state of sand, Journal of Geotechnical Engineering, Vol.122, No.6, pp.462 – 473.

Frost, J. D. and Jang, D. J. 2000. Evolution of sand microstructure during shearing, Journal of Geotechnical and Geoenvironmental Engineering, ASCE, Vol.126, No.2, pp.116-130.

Hird, C.C. and Hassona, F.A.K. 1990. Some factors affecting the liquefaction and flow of saturated sands in laboratory tests, Engineering Geology, Vol.28, pp.149-170.

Holtz, R.D. and Kovacs, W. 1981. An introduction to geotechnical engineering, Prentice-Hall, Inc., Englewood Cliffs, N.J., 733 pp.

Hvorslev, M.J. 1939. Torsion shear tests and their place in the determination of shearing resistance of soils, Proceedings of the American Society of Testing and Materials, Vol.39, pp.999-1022.

Infante Sedano, J.A. 1998. Constant volume ring shear test for sand, M.Sc. Thesis, Department of Civil Eng., University of Ottawa, Ottawa, Ontario.

Iverson N.R., Hooyer, T.S. and Baker, R.W. 1998. Ring shear studies of till deformation: Coulomb-plastic behavior and distributed strain in glacier beds, Journal of Glaciology, Vol.44, No.148, pp.634-642.

Murthy, T.G., Loukidis, D., Carraro, J.A.H., Prezzi, M. and Salgado, R. 2007. Undrained monotonic response of clean and silty sands, Geotechnique, Vol.57, No.3, pp.273-288.

Poorooshasb, H.B. 1989. Description of flow of sand using state parameters, Computers and Geotechniques, Vol.8, pp.195-218.

Poulos, J. 1981. The steady state of deformation, ASCE Journal of Geotechnical Engineering Division, Vol.107, No.GT5, pp.553-562.

Riemer, M. F. and Seed, R. B. 1997. Factors affecting apparent position of steady-state line, Journal of Geotechnical and Geo-environmental Engineering, Vo.123, No.3, pp.281-288.

Roscoe, K. H., Schofield, A. N., and Wroth, M. A. 1958. On the yielding of soils, Geotechnique, Vol.8, pp.22 – 53.

Sadrekarimi, A. 2009. "Development of a new ring shear device for investigating the critical state of sands," Ph.D. Thesis, University of Illinois at Urbana-Champaign.

Sadrekarimi, A. and Olson, S.M. 2009. A new ring shear device to measure the large displacement shearing behavior of sands, Geotechnical Testing Journal, ASTM, Vol.32, No.3.

Taylor, D.W. 1948. Fundamentals of Soil Mechanics, New York, John Wiley and Sons, 700 pp.

Verdugo, R. and Ishihara, K. 1996. The steady state of sandy soils, Soils and Foundations, Vol.36, No.2, pp.81-91.

Yamamuro, J.A., and Lade, P.V. 1997. Static liquefaction of very loose sands, Canadian Geotechnical Journal, Vol.34, pp.905–917.